

Possibility of the experimental study on semi-leptonic and non-leptonic $D_{(s)}^*$ weak decays

Hao Yang¹, Zhi-Qing Zhang^{1 *}, Peng Li^{2†}, You-Ya Yang¹

¹ *School of Physics, Henan University of Technology, Zhengzhou, Henan 450052, China*

² *Institute for Complexity Science, Henan University of Technology, Zhengzhou, Henan 450001, China*

(Dated: September 12, 2024)

Abstract

Just like other heavy flavor mesons, the weak decays of $D_{(s)}^*$ mesons can also provide a platform to check the Standard Model (SM), explore new physics (NP) and understand the mechanisms of weak interactions. At present, the theoretical and experimental researches on $D_{(s)}^*$ mesons are relatively limited. In addition to the dominant electromagnetic decays, the $D_{(s)}^*$ weak decays should also be feasible to explore the $D_{(s)}^*$ mesons. In this paper, we use the covariant light-front quark model (CLFQM) to study the branching ratios of the semi-leptonic decays $D_{(s)}^* \rightarrow P\ell^+\nu_\ell$ and the non-leptonic decays $D_{(s)}^* \rightarrow PP, PV$ with $P = \pi, K, \eta^{(\prime)}, V = \rho, K^*, \phi$ and $\ell = e, \mu$, which are within the range $10^{-13} \sim 10^{-6}$. Among these decays, the channels $D_s^{*+} \rightarrow \eta\ell^+\nu_\ell$ and $D_s^{*+} \rightarrow \eta\rho^+$ possess the largest branching ratios, which can reach up to 10^{-6} order. These decays are most likely to be accessible at the future high-luminosity experiments. One can find that the branching ratios $\mathcal{Br}(D_s^{*+} \rightarrow \eta\ell^+\nu_\ell) = 1.46 \times 10^{-6}$ and $\mathcal{Br}(D_s^{*+} \rightarrow \eta\rho^+) = 1.04 \times 10^{-6}$ correspond to tens of thousands of events in the e^+e^- collider experiments, such as the STCF, CEPC and FCC-ee, and tens of millions of events at the HL-LHC. In a word, it is feasible to study the $D_{(s)}^*$ meson weak decays in the future experiments. Furthermore, we also predict and discuss another two physical observations, that is, the longitudinal polarization fraction f_L and the forward-backward asymmetry A_{FB} , for our considered decays.

PACS numbers: 13.25.Hw, 12.38.Bx, 14.40.Nd

* zhangzhiqing@haut.edu.cn

† lipeng@haut.edu.cn

I. INTRODUCTION

In the 1970s and 1980s, Terentev and Bereshtsky proposed the light-front quark model (LFQM) [1, 2], which aims to deal with non-perturbable physical quantities such as decay constants and transition form factors [3–5]. However, the standard LFQM has trouble dealing with zero-mode contributions. To address this limitation, Jaus developed an improved model, the covariant light-front quark model (CLFQM)[6]. Compared with other quark-model approaches, the CLFQM has some unique advantages. First, the light-front wave functions used in this approach are independent of the hadron momentum and thus are manifestly Lorentz invariant. Moreover, the hadron spin is correctly constructed using the so-called Melosh rotation. Second, this model provides a relativistic treatment of the hadron. Since the final state meson at the maximum recoil point ($q^2 = 0$) or in heavy-to-light transitions can be highly relativistic, it is important to consider relativistic effects. Then it is expected that the non-relativistic quark model may not work well. Last, in the CLFQM, the spurious contributions, which are dependent on the orientation of the light-front, are just canceled by the zero-mode contributions, thereby the covariance of the current matrix elements lost in the previous standard KFQM is restored. This model has been successfully used in the study of non-leptonic and semi-leptonic meson decays [7–12].

The weak decays of the $D_{(s)}^*$ mesons provide another important platform and opportunities to understand the properties of the $D_{(s)}^*$ mesons, explore their decay mechanism and test the SM. Due to the small strength of the weak interactions, the $D_{(s)}^*$ weak decays are usually very rare processes. At present only several decay modes of $D_{(s)}^*$ mesons have been observed on experiments, that is, $D_{(s)}^* \rightarrow D_{(s)}\pi, D_{(s)}\gamma, D_{(s)}e^+e^-$. Very recently, along with the advancement of experimental techniques, the BESIII collaboration has reported the first experimental study of the purely leptonic decay $D_s^{*+} \rightarrow e^+\nu_e$ [13] with the branching ratio measured as $(2.1_{-0.9}^{+1.2} \pm 0.2) \times 10^{-5}$. Although the theoretical predictions about the $D_{(s)}^*$ properties are still relatively limited, and the information regarding the $D_{(s)}^*$ weak decays is still unavailable, the experimental progress of the investigation of $D_{(s)}^*$ mesons at various high energy collider experiments will provide more and more data on the $D_{(s)}^*$ meson decays, so the theoretical study of the $D_{(s)}^*$ weak decays should have broad prospects in the near future.

Assuming that the exclusive cross sections near threshold $\sigma(e^+e^- \rightarrow D^0\bar{D}^{*0}) \approx \sigma(e^+e^- \rightarrow D^+D^{*-}) \approx 4\text{nb}$ and $\sigma(e^+e^- \rightarrow D^{*0}\bar{D}^{*0}) \approx \sigma(e^+e^- \rightarrow D^{*+}D^{*-}) \approx 3\text{nb}$, more than 5×10^7 $D^{*\pm}$ meson events have been accumulated corresponding to a total integrated luminosity of 15.7fb^{-1} within the energy region $\sqrt{s} \in [4.085, 4.600]$ in BESIII experiments [14]. While it is not sufficient to explore the D^* meson weak decays. In the future, about 8×10^{10} D^{*0} and $D^{*\pm}$ events will be produced at the τ -charm factory (STCF) at a total integrated luminosity

of 10 ab^{-1} [15]. Given the charm quark fragmentation fractions $f(c \rightarrow D^{*+}) \approx 25\%$ and $f(c \rightarrow D^{*0}) \approx 23\%$ [16], more than 2×10^{10} D^{*0} and $D^{*\pm}$ mesons will be collected at SuperKEKB [17]. It is expected that about 10^{12} and 10^{13} Z^0 bosons will be available at the Circular Electron Positron Collider (CEPC) [18] and the Future Circular Collider (FCC-ee) [19] with a total integrated luminosity 20 ab^{-1} , respectively. Considering the branching ratios $\mathcal{B}r(Z^0 \rightarrow D^{*\pm}X) \approx \mathcal{B}r(Z^0 \rightarrow D^{*\pm}X) = (11.4 \pm 1.3)\%$ [20], more than 10^{11} and 10^{12} D^* mesons can be obtained at CEPC and FCC-ee, respectively. In addition, with the inclusive cross section $\sigma(pp \rightarrow D^{*+}X) = 784 \pm 4 \pm 87 \pm 118 \text{ } \mu\text{b}$ at the center of mass energy $\sqrt{s} = 13\text{TeV}$ measured by the LHCb [21], more than 2×10^{14} D^* mesons with a total integrated luminosity of 300fb^{-1} will be collected at the High Luminosity LHC (HL-LHC) experiments up to 2037 [22]. Assuming the exclusive cross sections near threshold $\sigma(e^+e^- \rightarrow D_s^+ D_s^{*-})$ and $\sigma(e^+e^- \rightarrow D_s^{*+} D_s^{*-})$ were measured as 1.0 nb and 0.2 nb [23–25], about 10^{10} $D_s^{*\pm}$ events corresponding to a data sample of 10 ab^{-1} will be available at STCF. Given the branching ratio $\mathcal{B}r(Z^0 \rightarrow c\bar{c}) = (12.03 \pm 0.21)\%$ and the fragmentation fraction $f(c \rightarrow D_s^*) \simeq 5.5\%$ [16], about 1.3×10^{10} and 6.6×10^{10} $D_s^{*\pm}$ events corresponding to 10^{12} and 5×10^{12} Z bosons will be collected at the future CEPC [18] and FCC-ee [19] experiments, respectively. Given the fragmentation fraction $f(c \rightarrow D_s^*) \simeq 5.5\%$ [16], about 5.5×10^9 D_s^* events corresponding to 5×10^{10} $c\bar{c}$ pairs can be collected in the future SuperKEKB experiments [17]. In addition, considering the inclusive cross section $\sigma(pp \rightarrow c\bar{c}X) = 2.4 \text{ mb}$ at the center-of-mass energy of $\sqrt{s} = 13 \text{ TeV}$ [21] and the charm quark fragmentation fraction $f(c \rightarrow D_s^*) \approx 5.5\%$, about 4×10^{13} D_s^* events corresponding to a data sample of 300 fb^{-1} can be collected at the LHCb [26].

In the semi-leptonic decays, the calculations of the hadronic matrix elements are crucial and can be characterized by several form factors [27], which can be extracted from data or obtained using some non-perturbative methods. The CLFQM as one of popular non-perturbative approaches has been successfully used to calculate the form factors [7, 8, 28–31]. As to the non-leptonic decays involving two hadrons in the final states, the related dynamics becomes more complex when the long distance interactions are involved. While for some non-leptonic decays governed by the tree operators, the corresponding matrix elements can be decomposed into the product of the decay constant and the transition form factor by means of the vacuum saturation hypothesis. Such factorization approach is verified to work well for the color-allowed decay modes and has been widely used in the analysis of the non-leptonic decays [27]. In conclusion, the form factors are of great significance for studying the semi-leptonic and non-leptonic weak decays. Many theoretical models, such as the QCD sum rules (QCDSR) [32, 33], the Bauer-Stech-Wirbel (BSW) model [34] and the Bethe-Salpeter (BS) method [35], have been also used to study the transition form factors. Combining the form factors with helicity amplitudes, besides the branching ratios, we also calculate another

two physical observables, namely the longitudinal polarization fraction f_L and the forward-backward asymmetry A_{FB} . These observables provide valuable insights into the underlying dynamics of the considered decay processes and important constraints on testing the SM.

The paper is organized as follows. The formalisms of the CLFQM, the hadronic matrix elements and the helicity amplitudes combined via form factors are listed in Sec. II. Besides the numerical results of the form factors of the transitions $D_{(s)}^* \rightarrow K, \pi, \eta_{q,s}$, the branching ratios, the longitudinal polarization fractions f_L and the forward-backward asymmetries A_{FB} for the corresponding decays are presented in Sec. III. Comparison with other theoretical results and relevant discussions are also included. The summary is given in Sec. IV. In Appendix A and B, some specific rules in the process of performing p^- integration as well as expressions for the form factor are collected, respectively.

II. FORMALISM

The form factors for the transitions $D_{(s)}^* \rightarrow P$ are defined as follows,

$$\begin{aligned} \langle P(P'') | V_\mu - A_\mu | D_{(s)}^*(P', \epsilon) \rangle = & \epsilon_{\mu\nu\alpha\beta} \epsilon^\nu q^\alpha P^\beta \frac{V^{D_{(s)}^* P}(q^2)}{m_{D_{(s)}^*} + m_P} - i 2 \frac{m_{D_{(s)}^*} \epsilon \cdot q}{q^2} q_\mu A_0^{D_{(s)}^* P}(q^2) \\ & - i \epsilon_\mu (m_{D_{(s)}^*} + m_P) A_1^{D_{(s)}^* P}(q^2) - i \frac{\epsilon \cdot q}{m_{D_{(s)}^*} + m_P} P_\mu A_2^{D_{(s)}^* P}(q^2) \\ & + i \frac{2m_{D_{(s)}^*} \epsilon \cdot q}{q^2} q_\mu A_3^{D_{(s)}^* P}(q^2), \end{aligned} \quad (1)$$

where $p = p' + p''$, $q = p' - p''$, ϵ is the polarization vector and the convention $\epsilon_{0123} = 1$

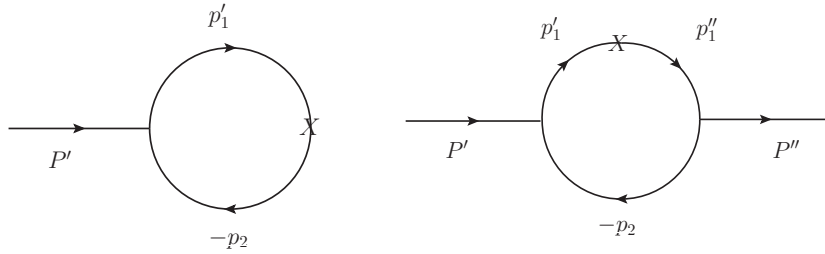


FIG. 1: Feynman diagrams for $D_{(s)}^*$ decay (left) and transition (right) amplitudes, where $P'^{(\prime\prime)}$ is the incoming (outgoing) meson momentum, $p_1'^{(\prime\prime)}$ is the quark momentum, p_2 is the anti-quark momentum and X denotes the vector or axial-vector transition vertex.

is adopted. In above equations, V_μ and A_μ are the corresponding vector and axial-vector currents, which are dominant contributions in the weak decays. The four-momentum of the initial (final) meson is $p' = p'_1 + p_2$ ($p'' = p'_1 + p_2$), where $p'^{(\prime\prime)}$ and p_2 are the momenta of the quark and antiquark inside the incoming (outgoing) meson. Following the convention and calculation rules for the form factors of the transition $J/\Psi \rightarrow D$ in Ref. [27], one can write

out the decay amplitude in the lowest order for the transition $D_{(s)}^* \rightarrow P$, whose Fynman diagram is shown in Fig.1,

$$\mathcal{B}_\mu^{D_{(s)}^* P} = -i^3 \frac{N_c}{(2\pi)^4} \int d^4 p'_1 \frac{h'_{D_{(s)}^*} (i h''_P)}{N'_1 N''_1 N_2} S_{\mu\nu}^{D_{(s)}^* P} \varepsilon^{*\nu}, \quad (2)$$

where $N_1'^{(n)} = p_1'^{(n)2} - m_1'^{(n)2}$, $N_2 = p_2^2 - m_2^2$ arise from the quark propagators, and the trace $S_{\mu\nu}^{D_{(s)}^* P}$ can be obtained directly using Lorentz contraction,

$$\begin{aligned} S_{\mu\nu}^{D_{(s)}^* P} &= \left(S_V^{D_{(s)}^* P} - S_A^{D_{(s)}^* P} \right)_{\mu\nu} \\ &= \text{Tr} \left[\left(\gamma_\nu - \frac{1}{W_V''} (p_1'' - p_2)_\nu \right) (p_1'' + m_1'') (\gamma_\mu - \gamma_\mu \gamma_5) (\not{p}'_1 + m'_1) \gamma_5 (-\not{p}_2 + m_2) \right]. \end{aligned} \quad (3)$$

Its specific expression is listed in Appendix B. The covariant vertex function $h'_{D_{(s)}^*}$ is defined as

$$h'_{D_{(s)}^*} = (M'^2 - M_0'^2) \sqrt{\frac{x_1 x_2}{N_c}} \frac{1}{\sqrt{2} \widetilde{M}_0'} \varphi', \quad (4)$$

where M' refers to $m_{D_{(s)}^*}$, M_0' is the kinetic invariant mass of the initial meson $D_{(s)}^*$ and can be expressed as the energies $e_i^{(i)}$ ($i = 1, 2$) of the constituent quark and anti-quark with masses (momentum fractions) being $m'_1(x_1)$ and $m_2(x_2)$, respectively. Their definitions including the denominator \widetilde{M}_0' are given as follows

$$\begin{aligned} M_0'^2 &= (e'_1 + e_2)^2 = \frac{p_\perp'^2 + m_1'^2}{x_1} + \frac{p_\perp^2 + m_2^2}{x_2}, \quad \widetilde{M}_0' = \sqrt{M_0'^2 - (m'_1 - m_2)^2}, \\ e_i^{(i)} &= \sqrt{m_i^{(i)2} + p_\perp'^2 + p_z'^2} \quad (i = 1, 2), \quad x_1 + x_2 = 1, \end{aligned} \quad (5)$$

where $p_z' = \frac{x_2 M_0'}{2} - \frac{m_2^2 + p_\perp'^2}{2x_2 M_0'}$. The phenomenological Gaussian-type wave function φ' depicts the light-front momentum distribution amplitude for the S-wave mesons,

$$\varphi' = \varphi'(x_2, p'_\perp) = 4 \left(\frac{\pi}{\beta'^2} \right)^{\frac{3}{4}} \sqrt{\frac{dp_z'}{dx_2}} \exp \left(-\frac{p_z'^2 + p_\perp'^2}{2\beta'^2} \right), \quad (6)$$

where β' is a phenomenological parameter and can be fixed by fitting the corresponding decay constant. The expressions of the vertex functions h_P'' for our considered pseudoscalar mesons are similar. After expanding the trace $S_{\mu\nu}^{D_{(s)}^* P}$ using the Lorentz contraction, then one can get the form factors $V^{D_{(s)}^* P}$, $A_0^{D_{(s)}^* P}$, $A_1^{D_{(s)}^* P}$ and $A_2^{D_{(s)}^* P}$ by matching to the coefficients given in Eq. (1). Their specific expressions are listed in Appendix B.

By combining the helicity amplitudes via the form factors, we can derive the differential

widths of the semi-leptonic decays $D_{(s)}^* \rightarrow P \ell \nu_\ell$,

$$\frac{d\Gamma_L}{dq^2} = \left(\frac{q^2 - m_\ell^2}{q^2}\right)^2 \frac{\sqrt{\lambda(m_{D_{(s)}^*}^2, m_P^2, q^2)} G_F^2 |V_{CKM}|^2}{384 m_{D_{(s)}^*}^3 \pi^3} \times \frac{1}{q^2} \left\{ 3m_\ell^2 \lambda(m_{D_{(s)}^*}^2, m_P^2, q^2) A_0^2(q^2) \right. \\ \left. + \frac{m_\ell^2 + 2q^2}{4m_P^2} \left| (m_{D_{(s)}^*}^2 - m_P^2 - q^2)(m_{D_{(s)}^*} + m_P) A_1(q^2) - \frac{\lambda(m_{D_{(s)}^*}^2, m_P^2, q^2)}{m_{D_{(s)}^*} + m_P} A_2(q^2) \right|^2 \right\}, \quad (7)$$

$$\frac{d\Gamma_\pm}{dq^2} = \left(\frac{q^2 - m_\ell^2}{q^2}\right)^2 \frac{\sqrt{\lambda(m_{D_{(s)}^*}^2, m_P^2, q^2)} G_F^2 |V_{CKM}|^2}{384 m_{D_{(s)}^*}^3 \pi^3} \\ \times \left\{ (m_\ell^2 + 2q^2) \lambda(m_{D_{(s)}^*}^2, m_P^2, q^2) \left| \frac{V(q^2)}{m_{D_{(s)}^*} + m_P} \mp \frac{(m_{D_{(s)}^*} + m_P) A_1(q^2)}{\sqrt{\lambda(m_{D_{(s)}^*}^2, m_P^2, q^2)}} \right|^2 \right\}, \quad (8)$$

where $\lambda(q^2) = \lambda(m_{D_{(s)}^*}^2, m_P^2, q^2) = (m_{D_{(s)}^*}^2 + m_P^2 - q^2)^2 - 4m_{D_{(s)}^*}^2 m_P^2$, and m_ℓ is the mass of the lepton ℓ . Although the electron and nucleon masses are significantly small, we do not ignore them in the calculations in order to check the mass effects. The combined transverse and total differential decay widths are defined as

$$\frac{d\Gamma_T}{dq^2} = \frac{d\Gamma_+}{dq^2} + \frac{d\Gamma_-}{dq^2}, \quad \frac{d\Gamma}{dq^2} = \frac{d\Gamma_L}{dq^2} + \frac{d\Gamma_T}{dq^2}. \quad (9)$$

For the $D_{(s)}^*$ decays, it is meaningful to define the longitudinal polarization fraction due to the existence of different polarizations

$$f_L = \frac{\Gamma_L}{\Gamma_L + \Gamma_+ + \Gamma_-}. \quad (10)$$

As to the forward-backward asymmetry, the analytical expression is defined as [36],

$$A_{FB} = \frac{\int_0^1 \frac{d\Gamma}{d\cos\theta} d\cos\theta - \int_{-1}^0 \frac{d\Gamma}{d\cos\theta} d\cos\theta}{\int_{-1}^1 \frac{d\Gamma}{d\cos\theta} d\cos\theta} = \frac{\int b_\theta(q^2) dq^2}{\Gamma_{D_{(s)}^*}}, \quad (11)$$

where θ is defined as the angle between the 3-momenta of the lepton ℓ and the initial meson in the rest frame of $\ell \nu_\ell$. The function $b_\theta(q^2)$ refers to the angle coefficient and its expression can be written as [36]

$$b_\theta(q^2) = \frac{G_F^2 |V_{CKM}|^2}{128 \pi^3 m_{D_{(s)}^*}^3} q^2 \sqrt{\lambda(q^2)} \left(1 - \frac{m_\ell^2}{q^2}\right)^2 \left[\frac{1}{2} (H_{V,+}^2 - H_{V,-}^2) + \frac{m_\ell^2}{q^2} (H_{V,0} H_{V,t}) \right], \quad (12)$$

where the helicity amplitudes for the $D_{(s)}^* \rightarrow P$ transitions are given as

$$H_{V,\pm}(q^2) = (m_{D_{(s)}^*} + m_P) A_1(q^2) \mp \frac{\sqrt{\lambda(q^2)}}{m_{D_{(s)}^*} + m_P} V(q^2), \\ H_{V,0}(q^2) = \frac{m_{D_{(s)}^*} + m_P}{2m_{D_{(s)}^*} \sqrt{q^2}} \left[- (m_{D_{(s)}^*}^2 - m_P^2 - q^2) A_1(q^2) + \frac{\lambda(q^2) A_2(q^2)}{(m_{D_{(s)}^*} + m_P)^2} \right], \\ H_{V,t}(q^2) = -\sqrt{\frac{\lambda(q^2)}{q^2}} A_0(q^2), \quad (13)$$

where the subscript V in each helicity amplitude refers to the $\gamma_\mu(1 - \gamma_5)$ current.

Based on the effective Hamiltonian, the amplitudes for the decays $D_{(s)}^* \rightarrow PM_1$ with $M_1 = \pi, K$ can be expressed as

$$\mathcal{A}(D_{(s)}^* \rightarrow PM_1) = \langle PM_1 | \mathcal{H}_{eff} | D_{(s)}^* \rangle = \frac{G_F}{\sqrt{2}} V_{uq_1}^* V_{cq_2} a_i \langle M_1 | J^\mu | 0 \rangle \langle P | J_\mu | D_{(s)}^* \rangle \quad (14)$$

where $q_{1,2} = s, d$, the combination of the Wilson coefficients $a_1 = C_1 + C_2/3$ and $a_2 = C_2 + C_2/3$. As to the specific decay channels, the amplitudes are given as

$$\mathcal{A}(D_s^{*+} \rightarrow \eta K^+) = -\sqrt{2} G_F V_{us} V_{cs}^* a_1 m_{D_s^*} (\epsilon \cdot p_K) f_K A_0^{D_s^* \eta_s} \sin \theta, \quad (15)$$

$$\mathcal{A}(D_s^{*+} \rightarrow \eta \pi^+) = -\sqrt{2} G_F V_{ud} V_{cs}^* a_1 m_{D_s^*} (\epsilon \cdot p_\pi) f_\pi A_0^{D_s^* \eta_s} \sin \theta, \quad (16)$$

$$\mathcal{A}(D^{*+} \rightarrow \eta K^+) = \sqrt{2} G_F V_{us} V_{cd}^* a_1 m_{D^*} (\epsilon \cdot p_K) f_K A_0^{D^* \eta_q} \cos \theta, \quad (17)$$

$$\mathcal{A}(D^{*+} \rightarrow \eta \pi^+) = \sqrt{2} G_F V_{ud} V_{cd}^* a_1 m_{D^*} (\epsilon \cdot p_\pi) f_\pi A_0^{D^* \eta_q} \cos \theta, \quad (18)$$

$$\mathcal{A}(D^{*0} \rightarrow \eta K^0) = \sqrt{2} G_F V_{us} V_{cd}^* a_1 m_{D^*} (\epsilon \cdot p_K) f_K A_0^{D^* \eta_q} \cos \theta, \quad (19)$$

$$\mathcal{A}(D_s^{*+} \rightarrow K^0 K^+) = \sqrt{2} G_F V_{us} V_{cd}^* a_1 m_{D_s^*} (\epsilon \cdot p_K) f_K A_0^{D_s^* K}, \quad (20)$$

$$\mathcal{A}(D_s^{*+} \rightarrow K^0 \pi^+) = \sqrt{2} G_F V_{ud} V_{cd}^* a_1 m_{D_s^*} (\epsilon \cdot p_\pi) f_\pi A_0^{D_s^* K}, \quad (21)$$

$$\mathcal{A}(D^{*+} \rightarrow \bar{K}^0 K^+) = \sqrt{2} G_F V_{us} V_{cs}^* a_1 m_{D^*} (\epsilon \cdot p_K) f_K A_0^{D^* K}, \quad (22)$$

$$\mathcal{A}(D^{*+} \rightarrow \bar{K}^0 \pi^+) = \sqrt{2} G_F V_{ud} V_{cs}^* m_{D^*} (\epsilon \cdot p_\pi) (a_1 f_\pi A_0^{D^* K} + a_2 f_K A_0^{D^* \pi}), \quad (23)$$

$$\mathcal{A}(D^{*0} \rightarrow \pi^- K^+) = \sqrt{2} G_F V_{us} V_{cd}^* a_1 m_{D^*} (\epsilon \cdot p_K) f_K A_0^{D^* \pi}, \quad (24)$$

$$\mathcal{A}(D^{*0} \rightarrow \pi^- \pi^+) = \sqrt{2} G_F V_{ud} V_{cd}^* a_1 m_{D^*} (\epsilon \cdot p_\pi) f_\pi A_0^{D^* \pi}, \quad (25)$$

$$\mathcal{A}(D^{*0} \rightarrow K^- K^+) = \sqrt{2} G_F V_{us} V_{cs}^* a_1 m_{D^*} (\epsilon \cdot p_K) f_K A_0^{D^* K}, \quad (26)$$

$$\mathcal{A}(D^{*0} \rightarrow K^- \pi^+) = \sqrt{2} G_F V_{ud} V_{cs}^* a_1 m_{D^*} (\epsilon \cdot p_\pi) f_\pi A_0^{D^* K}, \quad (27)$$

where ϵ is the polarization four vector of the $D_{(s)}^*$ meson, and θ is the mixing angle between the two flavor states η_s and η_q , which is defined as

$$\begin{pmatrix} \eta \\ \eta' \end{pmatrix} = \begin{pmatrix} \cos \theta & -\sin \theta \\ \sin \theta & \cos \theta \end{pmatrix} \begin{pmatrix} \eta_q \\ \eta_s \end{pmatrix}. \quad (28)$$

where the mixing angle θ has been well determined as $\theta = 39.3^\circ \pm 1.0^\circ$ [37]. In Eqs. (15) - (19), if one replaces the η with η' in the final states for each decay, the $-\sin \theta(\cos \theta)$ should be replaced with $\cos \theta(\sin \theta)$.

For the decays $D_{(s)}^* \rightarrow PV$ with V being ρ, K^*, ϕ , the hadronic matrix elements can be expressed as

$$\mathcal{A}(D_{(s)}^* \rightarrow PV) = \langle PV | \mathcal{H}_{eff} | D_{(s)}^* \rangle = \frac{G_F}{\sqrt{2}} V_{cq_1}^* V_{uq_2} a_{1,2} H_\lambda, \quad (29)$$

where $\lambda = 0, \mp$ denotes the helicity of vector meson, G_F is the Fermi coupling constant, $V_{cq_1}^* V_{uq_2}$ is the product of the CKM matrix elements, and the helicity amplitudes $\mathcal{H}_\lambda = \langle V | J^\mu | 0 \rangle \langle P | J_\mu | D_{(s)}^* \rangle$ are given as follows

$$\begin{aligned}
H_0 &\equiv \langle V(\varepsilon'_0, p_V) | \bar{q}_1 \gamma^\mu u | 0 \rangle \langle P(p_P) | \bar{c} \gamma_\mu (1 - \gamma_5) q_2 | D_{(s)}^*(\varepsilon_0, p_{D_{(s)}^*}) \rangle \\
&= \frac{if_V}{2m_{D_{(s)}^*}} \left[\left(m_{D_{(s)}^*}^2 - m_P^2 + m_V^2 \right) \left(m_{D_{(s)}^*} + m_P \right) A_1^{D_{(s)}^*P}(m_V^2) \right. \\
&\quad \left. + \frac{4m_{D_{(s)}^*}^2 p_c^2}{m_{D_{(s)}^*} + m_P} A_2^{D_{(s)}^*P}(m_V^2) \right], \tag{30}
\end{aligned}$$

$$\begin{aligned}
H_\mp &\equiv \langle V(\varepsilon'_\mp, p_V) | \bar{q}_1 \gamma^\mu u | 0 \rangle \langle P(p_P) | \bar{c} \gamma_\mu (1 - \gamma_5) q_2 | D_{(s)}^*(\varepsilon_\mp, p_{D_{(s)}^*}) \rangle \\
&= if_V m_V \left[- \left(m_{D_{(s)}^*} + m_P \right) A_1^{D_{(s)}^*P}(m_V^2) \mp \frac{2m_{D_{(s)}^*} p_c}{m_{D_{(s)}^*} + m_P} V^{D_{(s)}^*P}(m_V^2) \right]. \tag{31}
\end{aligned}$$

III. NUMERICAL RESULTS AND DISCUSSIONS

A. Transition Form Factors

TABLE I: The values of the input parameters.[9, 27, 38, 39]

Masses(GeV)	$m_c = 1.4$	$m_s = 0.37$	$m_{u,d} = 0.25$	$m_e = 0.000511$
	$m_\mu = 0.106$	$m_\tau = 1.777$	$m_\pi = 0.140$	$m_\rho = 0.770$
	$m_K = 0.494$	$m_{K^0} = 0.498$	$m_\eta = 0.548$	$m_{\eta'} = 0.958$
	$m_\phi = 1.019$	$m_{D^{*0}} = 2.007$	$m_{D^{*+}} = 2.01$	$m_{D_s^*} = 2.112$
CKM	$V_{cd} = 0.221 \pm 0.004$		$V_{us} = 0.2243 \pm 0.0008$	
	$V_{cs} = 0.975 \pm 0.006$		$V_{ud} = 0.97373 \pm 0.00031$	
Decay constants(GeV)	$f_\pi = 0.132$	$f_K = 0.16$	$f_{D^*} = 0.310_{-0.046}^{+0.046}$	
	$f_{\eta_q} = 0.141$	$f_{\eta_s} = 0.177$	$f_{D_s^*} = 0.301_{-0.045}^{+0.045}$	
	$f_{K^*} = 0.217$	$f_\rho = 0.209$	$f_\phi = 0.229$	
Shape parameters(GeV)	$\beta_{D^*} = 0.474_{-0.046}^{+0.042}$	$\beta_{D_s^*} = 0.466_{-0.046}^{+0.042}$	$\beta_K = 0.394_{-0.003}^{+0.003}$	
	$\beta_{\eta_q} = 0.374_{-0.03}^{+0.02}$	$\beta_{\eta_s} = 0.404_{-0.02}^{+0.01}$	$\beta_\pi = 0.328_{-0.004}^{+0.002}$	
Full widths	$\Gamma_{D^{*0}} = (55.9_{-5.4}^{+5.9})\text{KeV}$	$\Gamma_{D^{*+}} = (83.4 \pm 1.8)\text{KeV}$	$\Gamma_{D_s^{*+}} = (121.9_{-52.2}^{+69.6})\text{eV}$	

The input parameters, such as the constituent quark masses, the masses of the initial and the final mesons, the Cabibbo-Kobayashi-Maskawa (CKM) matrix elements, the shape parameters fitted by the decay constants, and $D_{(s)}^*$ meson lifes and so on are listed in Table I.

Based on the input parameters given in Table I, one can obtain the numerical results of the transition form factors at $q^2 = 0$ shown in Tables II and III. The uncertainties are from the shape parameters of the initial and final state mesons.

In Table II, we compare the numerical values of the form factors at maximum recoil ($q^2 = 0$) with those obtained within Ref. [38]. It is found that our predictions for the form factors of the transitions $D^* \rightarrow K, \pi$ and $D_s^* \rightarrow K$ are comparable with the previous light front quark model calculations [38] within errors. The difference between these two works is partially caused by the input parameters.

TABLE II: Numerical values of the transition form factors $D^* \rightarrow K, \pi$ and $D_s^* \rightarrow K$ at $q^2 = 0$, together with other theoretical results.

Transitions	Ref.		V	A_0	A_1	A_2
$D^* \rightarrow K$	This work	$F(0)$	$0.96^{+0.01}_{-0.02}$	$0.64^{+0.01}_{-0.02}$	$0.78^{+0.01}_{-0.02}$	$0.40^{+0.01}_{-0.02}$
	Ref.[38]		1.04	0.78	0.85	0.68
		$F(q_{max}^2)$	$0.98^{+0.02}_{-0.01}$	$0.75^{+0.03}_{-0.00}$	$0.88^{+0.02}_{-0.01}$	$0.45^{+0.02}_{-0.02}$
		a	$0.35^{+0.02}_{-0.03}$	$0.26^{+0.01}_{-0.01}$	$0.22^{+0.00}_{-0.01}$	$0.30^{+0.02}_{-0.02}$
		b	$0.57^{+0.06}_{-0.05}$	$0.04^{+0.01}_{-0.01}$	$0.03^{+0.01}_{-0.01}$	$0.22^{+0.01}_{-0.01}$
$D^* \rightarrow \pi$	This work	$F(0)$	$0.77^{+0.02}_{-0.02}$	$0.57^{+0.01}_{-0.01}$	$0.75^{+0.00}_{-0.01}$	$0.37^{+0.01}_{-0.01}$
	Ref.[38]		0.92	0.68	0.74	0.61
		$F(q_{max}^2)$	$0.57^{+0.02}_{-0.02}$	$0.74^{+0.02}_{-0.01}$	$0.92^{+0.01}_{-0.00}$	$0.37^{+0.01}_{-0.01}$
		a	$0.29^{+0.04}_{-0.05}$	$0.31^{+0.03}_{-0.01}$	$0.25^{+0.02}_{-0.01}$	$0.31^{+0.06}_{-0.03}$
		b	$0.80^{+0.11}_{-0.09}$	$0.07^{+0.01}_{-0.01}$	$0.04^{+0.01}_{-0.01}$	$0.34^{+0.02}_{-0.01}$
$D_s^* \rightarrow K$	This work	$F(0)$	$0.98^{+0.01}_{-0.01}$	$0.53^{+0.02}_{-0.03}$	$0.66^{+0.02}_{-0.03}$	$0.31^{+0.02}_{-0.03}$
	Ref.[38]		1.04	0.78	0.85	0.68
		$F(q_{max}^2)$	$0.80^{+0.01}_{-0.00}$	$0.60^{+0.03}_{-0.02}$	$0.74^{+0.03}_{-0.02}$	$0.30^{+0.03}_{-0.02}$
		a	$0.25^{+0.04}_{-0.05}$	$0.26^{+0.01}_{-0.02}$	$0.24^{+0.01}_{-0.01}$	$0.23^{+0.04}_{-0.05}$
		b	$1.06^{+0.13}_{-0.11}$	$0.11^{+0.02}_{-0.02}$	$0.08^{+0.02}_{-0.01}$	$0.35^{+0.02}_{-0.02}$

All the calculations are carried out within the $q^+ = 0$ reference frame, where the form factors can only be obtained at spacelike momentum transfers $q^2 = -q_\perp^2 \leq 0$. Those parameterized form factors are extrapolated from the space-like region to the time-like region by using following expression,

$$F(q^2) = \frac{F(0)}{1 - aq^2/m^2 + bq^4/m^4}, \quad (32)$$

where $F(q^2)$ denotes different form factors $V(q^2)$, $A_0(q^2)$, $A_1(q^2)$ and $A_2(q^2)$, and m represents the initial meson mass. The values of a and b can be obtained by performing a 3-parameter fit to the form factors in the range $-15\text{GeV}^2 \leq q^2 \leq 0$. We plot the q^2 -dependence of the form factors of the transitions $D_{(s)}^* \rightarrow P$ shown in Fig. 2.

TABLE III: Form factors of the transitions $D^* \rightarrow \eta_q$ and $D_s^* \rightarrow \eta_s$ in the CLFQM.

$D^* \rightarrow \eta_q$				
	V	A_0	A_1	A_2
$F(0)$	$0.96^{+0.02}_{-0.02}$	$0.56^{+0.01}_{-0.02}$	$0.67^{+0.01}_{-0.02}$	$0.36^{+0.01}_{-0.02}$
$F(q_{max}^2)$	$0.95^{+0.02}_{-0.02}$	$0.64^{+0.02}_{+0.01}$	$0.75^{+0.02}_{-0.01}$	$0.39^{+0.02}_{-0.02}$
a	$0.33^{+0.02}_{-0.03}$	$0.25^{+0.01}_{-0.01}$	$0.21^{+0.00}_{-0.01}$	$0.27^{+0.02}_{-0.03}$
b	$0.66^{+0.07}_{-0.06}$	$0.05^{+0.01}_{-0.01}$	$0.03^{+0.01}_{-0.01}$	$0.23^{+0.01}_{-0.01}$
$D_s^* \rightarrow \eta_s$				
	V	A_0	A_1	A_2
$F(0)$	$1.17^{+0.00}_{-0.02}$	$0.63^{+0.01}_{-0.02}$	$0.70^{+0.01}_{-0.02}$	$0.45^{+0.02}_{-0.03}$
$F(q_{max}^2)$	$1.17^{+0.02}_{-0.00}$	$0.68^{+0.03}_{-0.02}$	$0.75^{+0.02}_{-0.01}$	$0.47^{+0.03}_{-0.03}$
a	$0.28^{+0.04}_{-0.05}$	$0.31^{+0.01}_{-0.01}$	$0.29^{+0.00}_{-0.01}$	$0.29^{+0.03}_{-0.03}$
b	$0.95^{+0.12}_{-0.10}$	$0.11^{+0.02}_{-0.02}$	$0.09^{+0.02}_{-0.02}$	$0.38^{+0.03}_{-0.02}$

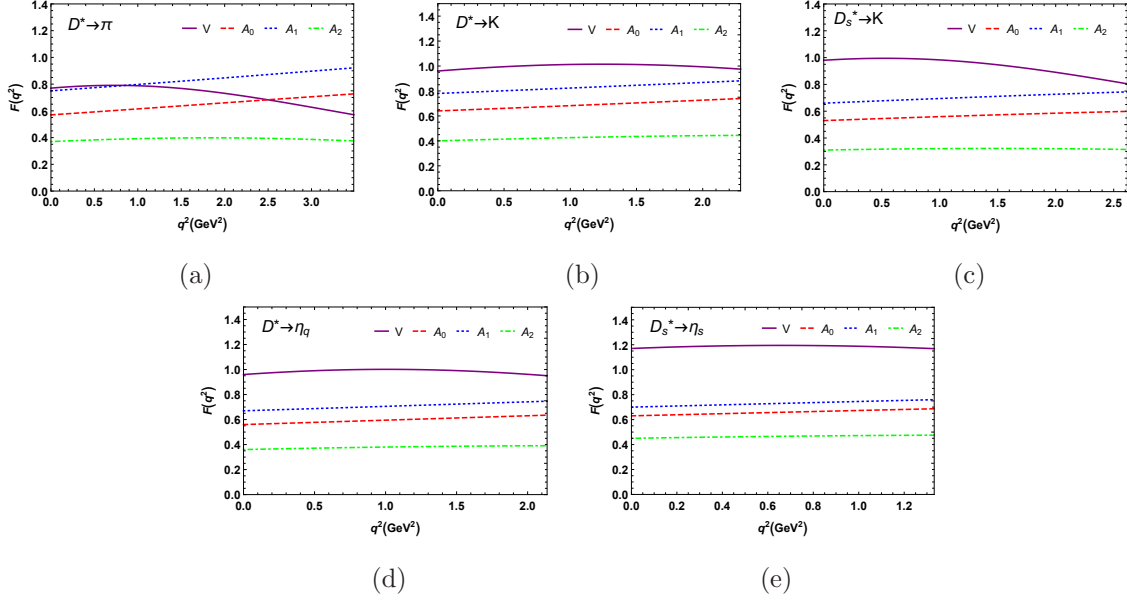


FIG. 2: Form factors $V(q^2)$, $A_0(q^2)$, $A_1(q^2)$, $A_2(q^2)$ of the transitions $D_{(s)}^{*0} \rightarrow \pi, K, \eta_q, \eta_s$.

B. Semi-leptonic decays

Based the form factors and the helicity amplitudes provided in the previous section, the branching ratios of the semi-leptonic decays $D_{(s)}^{*0(+)} \rightarrow P^{-(0)} \ell^+ \nu_\ell$ can be obtained and listed in Table IV, where the first error arises from the decay widths of $D_{(s)}^*$, the second uncertainty is from the shape parameters of the initial and final mesons.

TABLE IV: The branching ratios of the semi-leptonic decays $D_{(s)}^{*0(+)} \rightarrow P^{-(0)} \ell^+ \nu_\ell$.

	$10^{-9} \times \mathcal{B}r(D^{*0} \rightarrow \pi^- e^+ \nu_e)$	$10^{-9} \times \mathcal{B}r(D^{*0} \rightarrow \pi^- \mu^+ \nu_\mu)$	$10^{-9} \times \mathcal{B}r(D^{*0} \rightarrow K^- e^+ \nu_e)$	$10^{-9} \times \mathcal{B}r(D^{*0} \rightarrow K^- \mu^+ \nu_\mu)$
This work	$2.79^{+0.30+0.21}_{-0.27-0.03}$	$2.64^{+0.28+0.19}_{-0.25-0.04}$	$7.93^{+0.84+0.07}_{-0.76-0.36}$	$7.53^{+0.81+0.07}_{-0.72-0.34}$
	$10^{-9} \times \mathcal{B}r(D^{*+} \rightarrow \pi^0 e^+ \nu_e)$	$10^{-10} \times \mathcal{B}r(D^{*+} \rightarrow \pi^0 \mu^+ \nu_\mu)$	$10^{-14} \times \mathcal{B}r(D^{*+} \rightarrow \pi^0 \tau^+ \nu_\tau)$	$10^{-14} \times \mathcal{B}r(D^{*0} \rightarrow \pi^- \tau^+ \nu_\tau)$
This work	$1.00^{+0.02+0.07}_{-0.02-0.01}$	$9.50^{+0.21+0.69}_{-0.20-0.12}$	$2.25^{+0.05+0.06}_{-0.05-0.04}$	$4.96^{+0.53+0.14}_{-0.47-0.08}$
	$10^{-9} \times \mathcal{B}r(D^{*+} \rightarrow \bar{K}^0 e^+ \nu_e)$	$10^{-9} \times \mathcal{B}r(D^{*+} \rightarrow \bar{K}^0 \mu^+ \nu_\mu)$	$10^{-7} \times \mathcal{B}r(D_s^{*+} \rightarrow K^0 e^+ \nu_e)$	$10^{-7} \times \mathcal{B}r(D_s^{*+} \rightarrow K^0 \mu^+ \nu_\mu)$
This work	$5.29^{+0.12+0.05}_{-0.11-0.24}$	$5.03^{+0.11+0.05}_{-0.11-0.23}$	$1.97^{+0.21+0.06}_{-0.16-0.09}$	$1.87^{+0.20+0.06}_{-0.16-0.09}$
	$10^{-11} \times \mathcal{B}r(D^{*+} \rightarrow \eta e^+ \nu_e)$	$10^{-11} \times \mathcal{B}r(D^{*+} \rightarrow \eta \mu^+ \nu_\mu)$	$10^{-12} \times \mathcal{B}r(D^{*+} \rightarrow \eta' e^+ \nu_e)$	$10^{-12} \times \mathcal{B}r(D^{*+} \rightarrow \eta' \mu^+ \nu_\mu)$
This work	$5.03^{+0.11+0.18}_{-0.11-0.08}$	$4.79^{+0.11+0.17}_{-0.10-0.08}$	$7.58^{+0.17+0.20}_{-0.16-0.16}$	$7.06^{+0.16+0.27}_{-0.15-0.16}$
	$10^{-6} \times \mathcal{B}r(D_s^{*+} \rightarrow \eta e^+ \nu_e)$	$10^{-6} \times \mathcal{B}r(D_s^{*+} \rightarrow \eta \mu^+ \nu_\mu)$	$10^{-7} \times \mathcal{B}r(D_s^{*+} \rightarrow \eta' e^+ \nu_e)$	$10^{-7} \times \mathcal{B}r(D_s^{*+} \rightarrow \eta' \mu^+ \nu_\mu)$
This work	$1.46^{+0.16+0.03}_{-0.12-0.09}$	$1.41^{+0.15+0.02}_{-0.12-0.09}$	$5.08^{+0.55+0.10}_{-0.42-0.37}$	$4.80^{+0.52+0.10}_{-0.40-0.36}$

The branching ratios of the semi-leptonic $D_s^{*+} \rightarrow P\ell^+\nu_\ell$ decays are in the order of $10^{-7} \sim 10^{-6}$, which are much larger than those of the semi-leptonic $D^{*0(+)} \rightarrow P^{-(0)}\ell^+\nu_\ell$ decays within the range $10^{-12} \sim 10^{-9}$. It is mainly because that the decay width of the meson D_s^* is much more small than that of the meson D^* . In these semi-leptonic D_s^* decays, the decays $D_s^{*+} \rightarrow \eta\ell^+\nu_\ell$ have the largest branching ratios, which can be detected by the present experiments. While the branching ratios of the decays $D_s^{*+} \rightarrow \eta'\ell^+\nu_\ell$ are about three times smaller than those of the decays $D_s^{*+} \rightarrow \eta\ell^+\nu_\ell$. It is mainly because the smaller phase space. Although another two semi-leptonic D_s^* decays $D_s^{*+} \rightarrow K^0\ell^+\nu_\ell$ induced by the $c \rightarrow d$ transition have much smaller CKM matrix element V_{cd} than V_{cs} , the large phase space can reduce the gap of the branching ratios between the decays $D_s^{*+} \rightarrow K^0\ell^+\nu_\ell$ and $D_s^{*+} \rightarrow \eta'\ell^+\nu_\ell$. Since the τ lepton mass is much greater than the e and μ lepton masses, the τ can only produce through the decays $D^{*0(+)} \rightarrow \pi^{-(0)}\tau^+\nu_\tau$ with tiny branching ratios, which are only within 10^{-14} order. In a word, these considered semi-leptonic D_s^* decays have large branching ratios, which are larger than 10^{-7} order even can reach up to 10^{-6} order. So they are most likely to be detected by the future high-luminosity experiments, such as the Super Tau-Charm Factory (STCF), BESIII and LHCb. Furthermore, it is meaningful to define the ratios of the branching fractions, which can be estimated through the total widths of the initial mesons and the CKM matrix elements, for example,

$$\frac{\mathcal{B}r(D_s^{*+} \rightarrow \eta e^+\nu_e)}{\mathcal{B}r(D^{*+} \rightarrow \eta e^+\nu_e)} \approx \frac{2V_{cs}^2\Gamma_{D^{*+}}}{V_{cd}^2\Gamma_{D_s^{*+}}} \approx 2.7 \times 10^4, \quad (33)$$

$$\frac{\mathcal{B}r(D_s^{*+} \rightarrow K^0 e^+\nu_e)}{\mathcal{B}r(D^{*+} \rightarrow \bar{K}^0 e^+\nu_e)} \approx \frac{V_{cd}^2\Gamma_{D^{*+}}}{V_{cs}^2\Gamma_{D_s^{*+}}} \approx 35. \quad (34)$$

These ratios are consistent with the results calculated from the branching ratios given in Table IV, which can be tested in the future experiments.

C. Physical observables

For our considered semi-leptonic decays $D_{(s)}^{*0(+)} \rightarrow P^{-(0)}\ell^+\nu_\ell$, we define two additional physical observables, namely the forward-backward asymmetry A_{FB} and the longitudinal polarization fraction f_L , to account for the impact of lepton mass and provide more detailed physical picture. The results of these two physical observables are listed in Tables V and VI, respectively. Furthermore, in Figs. 3 and 4, we also display the q^2 -dependences of the forward-backward asymmetries A_{FB} and the differential decay rates $d\Gamma_{(L)}/dq^2$, respectively.

TABLE V: The forward-backward asymmetries A_{FB} for the decays $D_{(s)}^{*0(+)} \rightarrow P^{-(0)} \ell^+ \nu_\ell$, where the uncertainties are from the shape parameters of the initial and final mesons, respectively.

Channel	$D^{*0} \rightarrow \pi^- e^+ \nu_e$	$D^{*0} \rightarrow \pi^- \mu^+ \nu_\mu$	$D^{*0} \rightarrow K^- e^+ \nu_e$	$D^{*0} \rightarrow K^- \mu^+ \nu_\mu$
A_{FB}	$-0.033^{+0.003+0.001}_{-0.004-0.001}$	$-0.033^{+0.003+0.001}_{-0.004-0.001}$	$-0.148^{+0.014+0.007}_{-0.016-0.003}$	$-0.149^{+0.014+0.007}_{-0.016-0.003}$
Channel	$D^{*+} \rightarrow \pi^0 e^+ \nu_e$	$D^{*+} \rightarrow \pi^0 \mu^+ \nu_\mu$	$D^{*+} \rightarrow \pi^0 \tau^+ \nu_\tau$	$D^{*0} \rightarrow \pi^- \tau^+ \nu_\tau$
A_{FB}	$-0.031^{+0.001+0.001}_{-0.001-0.001}$	$-0.031^{+0.001+0.001}_{-0.001-0.001}$	$0.092^{+0.001+0.001}_{-0.016-0.001}$	$0.093^{+0.009+0.001}_{-0.009-0.003}$
Channel	$D^{*+} \rightarrow \bar{K}^0 e^+ \nu_e$	$D^{*+} \rightarrow \bar{K}^0 \mu^+ \nu_\mu$	$D_s^{*+} \rightarrow K^0 e^+ \nu_e$	$D_s^{*+} \rightarrow K^0 \mu^+ \nu_\mu$
A_{FB}	$-0.113^{+0.002+0.005}_{-0.002-0.003}$	$-0.114^{+0.002+0.005}_{-0.003-0.003}$	$-0.161^{+0.013+0.009}_{-0.018-0.007}$	$-0.162^{+0.013+0.009}_{-0.018-0.007}$
Channel	$D^{*+} \rightarrow \eta e^+ \nu_e$	$D^{*+} \rightarrow \eta \mu^+ \nu_\mu$	$D^{*+} \rightarrow \eta' e^+ \nu_e$	$D^{*+} \rightarrow \eta' \mu^+ \nu_\mu$
A_{FB}	$-0.184^{+0.004+0.009}_{-0.004-0.007}$	$-0.184^{+0.004+0.009}_{-0.004-0.007}$	$-0.166^{+0.004+0.008}_{-0.004-0.006}$	$-0.164^{+0.003+0.008}_{-0.004-0.006}$
Channel	$D_s^{*+} \rightarrow \eta e^+ \nu_e$	$D_s^{*+} \rightarrow \eta \mu^+ \nu_\mu$	$D_s^{*+} \rightarrow \eta' e^+ \nu_e$	$D_s^{*+} \rightarrow \eta' \mu^+ \nu_\mu$
A_{FB}	$-0.213^{+0.018+0.010}_{-0.023-0.003}$	$-0.213^{+0.018+0.010}_{-0.023-0.003}$	$-0.200^{+0.017+0.009}_{-0.022-0.003}$	$-0.198^{+0.017+0.009}_{-0.022-0.003}$

For these decays, we find that the values of the forward-backward asymmetries A_{FB}^μ and A_{FB}^e are almost equal to each other. It is noted that the dominant contributions to the A_{FB} for these decays arise from the terms proportional to $(H_{V,+}^2 - H_{V,-}^2)$ in Eq. (12). The A_{FB} of the decays $D^{*0(+)} \rightarrow \pi^{-(0)} \tau^+ \nu_\tau$ is about 3 times larger than those of the decays $D^{*0(+)} \rightarrow \pi^{-(0)} \ell^+ \nu_\ell$ in magnitude with minus signs. In Fig. 3, one can find that the channel $D^{*0} \rightarrow \pi^- \tau^+ \nu_\tau$ has opposite sign for the q^2 -dependence of the forward-backward asymmetry compared to those of the semileptonic decays $D^{*0} \rightarrow \pi^- \ell^+ \nu_\ell$. There exist the similar situation between the decays $D^{*+} \rightarrow \pi^0 \tau^+ \nu_\tau$ and $D^{*+} \rightarrow \pi^0 \ell^+ \nu_\ell$. The q^2 -dependences of the forward-backward asymmetries for the decays $D^{*+} \rightarrow P^0 \ell^+ \nu_\ell$ are similar to those for the decays $D_s^{*+} \rightarrow P^0 \ell^+ \nu_\ell$, which are not listed for simplicity.

In Table VI, we can clearly find that the longitudinal polarization fractions f_L between the decays $D_{(s)}^{*0(+)} \rightarrow P^{-(0)} e^+ \nu_e$ and $D_{(s)}^{*0(+)} \rightarrow P^{-(0)} \mu^+ \nu_\mu$ are very close to each other, that is

$$f_L(D_{(s)}^{*0(+)} \rightarrow P^{-(0)} e^+ \nu_e) \sim f_L(D_{(s)}^{*0(+)} \rightarrow P^{-(0)} \mu^+ \nu_\mu), \quad (35)$$

which reflects the lepton flavor universality (LFU).

TABLE VI: The longitudinal polarization fraction f_L for the decays $D_{(s)}^{*0(+)} \rightarrow P^{-(0)} \ell^+ \nu_\ell$ in Region 1 and Region 2.

Observables	Region 1	Region 2	Total	Observables	Region 1	Region 2	Total
$f_L(D^{*0} \rightarrow \pi^- e^+ \nu_e)$	0.96	0.82	0.93	$f_L(D^{*0} \rightarrow \pi^- \mu^+ \nu_\mu)$	0.96	0.82	0.93
$f_L(D^{*0} \rightarrow K^- e^+ \nu_e)$	0.82	0.52	0.71	$f_L(D^{*0} \rightarrow K^- \mu^+ \nu_\mu)$	0.81	0.52	0.71
$f_L(D^{*+} \rightarrow \pi^0 e^+ \nu_e)$	0.68	0.60	0.67	$f_L(D^{*+} \rightarrow \pi^0 \mu^+ \nu_\mu)$	0.68	0.60	0.67
$f_L(D^{*+} \rightarrow \eta e^+ \nu_e)$	0.77	0.49	0.67	$f_L(D^{*+} \rightarrow \eta \mu^+ \nu_\mu)$	0.76	0.49	0.66
$f_L(D^{*+} \rightarrow \eta' e^+ \nu_e)$	0.72	0.44	0.60	$f_L(D^{*+} \rightarrow \eta' \mu^+ \nu_\mu)$	0.71	0.44	0.59
$f_L(D^{*+} \rightarrow \bar{K}^0 e^+ \nu_e)$	0.66	0.36	0.54	$f_L(D^{*+} \rightarrow \bar{K}^0 \mu^+ \nu_\mu)$	0.65	0.36	0.53
$f_L(D_s^{*+} \rightarrow K^0 e^+ \nu_e)$	0.81	0.53	0.71	$f_L(D_s^{*+} \rightarrow K^0 \mu^+ \nu_\mu)$	0.80	0.53	0.70
$f_L(D_s^{*+} \rightarrow \eta e^+ \nu_e)$	0.74	0.48	0.64	$f_L(D_s^{*+} \rightarrow \eta \mu^+ \nu_\mu)$	0.73	0.48	0.63
$f_L(D_s^{*+} \rightarrow \eta' e^+ \nu_e)$	0.70	0.43	0.58	$f_L(D_s^{*+} \rightarrow \eta' \mu^+ \nu_\mu)$	0.69	0.43	0.57

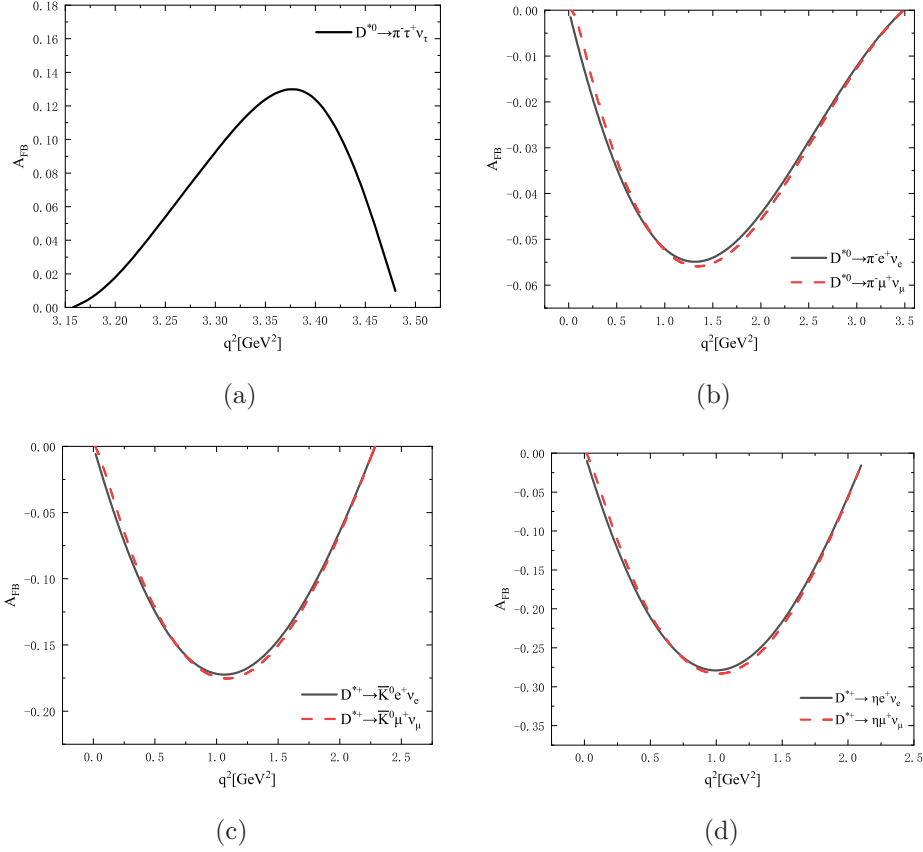


FIG. 3: The q^2 -dependences of the forward-backward asymmetries A_{FB} for the decays $D^{*0} \rightarrow \pi^- \tau^+ \nu_\tau$ (a), $D^{*0} \rightarrow \pi^- \ell^+ \nu_\ell$ (b), $D^{*+} \rightarrow \bar{K}^0 \ell^+ \nu_\ell$ (c) and $D^{*+} \rightarrow \eta \ell^+ \nu_\ell$ (d), respectively.

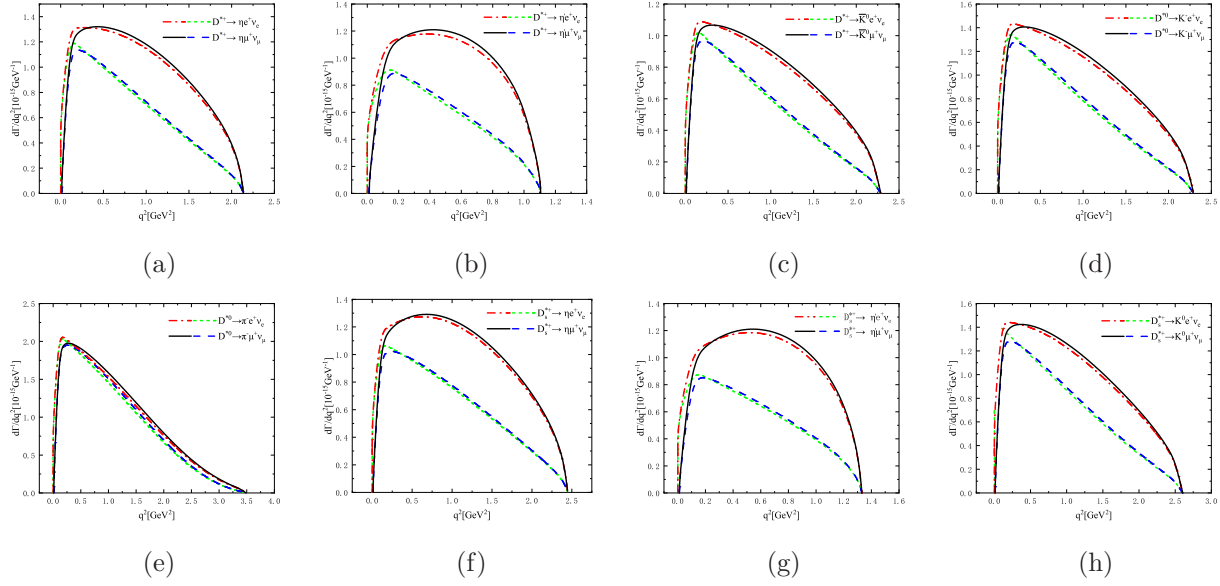


FIG. 4: The q^2 dependences of differential decay rates $d\Gamma/dq^2$ and $d\Gamma^L/dq^2$ for the decays $D_{(s)}^{*0(+)} \rightarrow P^{-(0)}\ell^+\nu_\ell$.

In order to investigate the dependences of the polarizations on the different q^2 , we divide the full energy region into two segments for each decay and calculate the longitudinal polarization fractions accordingly. Region 1 is defined as $m_\ell^2 < q^2 < \frac{(m_{D(s)}^* - m_P)^2 + m_\ell^2}{2}$ and Region 2 is $\frac{(m_{D(s)}^* - m_P)^2 + m_\ell^2}{2} < q^2 < (m_{D(s)}^* - m_P)^2$. Obviously, the longitudinal polarization fraction in Region 1 is larger than that in Region 2 for each decay, which can be found in Table VI. Furthermore, in each group of decays with the same initial meson, the longitudinal polarization fractions f_L for the decays induced by the $c \rightarrow d\ell^+\nu_\ell$ transition are always larger than those of the decays induced by the $c \rightarrow s\ell^+\nu_\ell$. For the decays $D^{*0(+)} \rightarrow \pi^{-(0)}\tau^+\nu_\tau$, the longitudinal polarization fraction f_L is only 0.43, which is much less than those of the decays $D^{*0(+)} \rightarrow \pi^{-(0)}\ell^+\nu_\ell$ because of $m_\tau \gg m_{e,\mu}$. A special emphasis is placed on the longitudinal polarizations for the decays $D^{*0} \rightarrow \pi^-\ell^+\nu_\ell$ shown in Fig. 4(e), which are absolutely dominant and very different from those for other channels. These results can be validated by the future high-luminosity experiments.

D. Non-leptonic decays

The decay rates of the nonleptonic weak decays $D_{(s)}^* \rightarrow PM$ with M standing for a pseudoscalar meson (π, K) or a vector meson (ρ, K^*, ϕ) can be written as [38]

$$\mathcal{B}r(D_{(s)}^* \rightarrow PM) = \frac{p_{cm}}{24\pi m_{D(s)}^* \Gamma_{D(s)}^*} |\mathcal{A}(D_{(s)}^* \rightarrow PM)|^2,$$

where p_{cm} represents the three-momentum of the final meson P in the rest frame of $D_{(s)}^*$, $m_{D_{(s)}^*}$ and $\Gamma_{D_{(s)}^*}$ are the mass and the decay width of the $D_{(s)}^*$ meson, respectively.

TABLE VII: Branching ratios of the non-leptonic weak decays $D^* \rightarrow PM$. The results obtained from the naive factorization (NF) approach [38] are also listed for comparison.

	$10^{-9} \times \mathcal{B}r(D^{*0} \rightarrow K^- \rho^+)$	$10^{-10} \times \mathcal{B}r(D^{*0} \rightarrow K^- K^{*+})$	$10^{-10} \times \mathcal{B}r(D^{*0} \rightarrow K^- \pi^+)$	$10^{-11} \times \mathcal{B}r(D^{*0} \rightarrow K^- K^+)$
This work	$5.13^{+0.55+0.05}_{-0.49-0.16}$	$2.41^{+0.26+0.03}_{-0.23-0.09}$	$4.67^{+0.49+0.17}_{-0.45-0.29}$	$2.95^{+0.32+0.11}_{-0.28-0.19}$
[38]	2.9	—	7.3	—
	$10^{-12} \times \mathcal{B}r(D^{*0} \rightarrow \eta \phi)$	$10^{-12} \times \mathcal{B}r(D^{*0} \rightarrow \eta' \phi)$	$10^{-13} \times \mathcal{B}r(D^{*0} \rightarrow \eta K^0)$	$10^{-13} \times \mathcal{B}r(D^{*0} \rightarrow \eta' K^0)$
This work	$8.33^{+0.95+1.4}_{-0.85-1.1}$	$1.65^{+0.17+0.20}_{-0.16-0.27}$	$3.32^{+0.35+0.11}_{-0.31-0.19}$	$1.08^{+0.12+0.02}_{-0.10-0.04}$
	$10^{-11} \times \mathcal{B}r(D^{*0} \rightarrow \pi^- \pi^+)$	$10^{-12} \times \mathcal{B}r(D^{*0} \rightarrow \pi^- K^+)$	$10^{-11} \times \mathcal{B}r(D^{*0} \rightarrow \pi^0 \phi)$	$10^{-13} \times \mathcal{B}r(D^{*0} \rightarrow \pi^0 K^0)$
This work	$2.42^{+0.26+0.04}_{-0.23-0.10}$	$1.59^{+0.17+0.03}_{-0.15-0.07}$	$2.59^{+0.28+0.39}_{-0.25-0.35}$	$8.04^{+0.86+0.15}_{-0.77-0.34}$
	$10^{-9} \times \mathcal{B}r(D^{*+} \rightarrow \bar{K}^0 \rho^+)$	$10^{-10} \times \mathcal{B}r(D^{*+} \rightarrow \bar{K}^0 K^{*+})$	$10^{-11} \times \mathcal{B}r(D^{*+} \rightarrow \bar{K}^0 \pi^+)$	$10^{-11} \times \mathcal{B}r(D^{*+} \rightarrow \bar{K}^0 K^+)$
This work	$3.44^{+0.08+0.03}_{-0.07-0.11}$	$1.62^{+0.04+0.02}_{-0.03-0.06}$	$9.79^{+0.22+0.52}_{-0.21-0.80}$	$2.07^{+0.04+0.08}_{-0.04-0.13}$
[38]	0.83	—	16	—
	$10^{-11} \times \mathcal{B}r(D^{*+} \rightarrow \eta \rho^+)$	$10^{-12} \times \mathcal{B}r(D^{*+} \rightarrow \eta K^{*+})$	$10^{-12} \times \mathcal{B}r(D^{*+} \rightarrow \eta \pi^+)$	$10^{-13} \times \mathcal{B}r(D^{*+} \rightarrow \eta K^+)$
This work	$4.17^{+0.09+0.10}_{-0.09-0.09}$	$1.32^{+0.03+0.01}_{-0.03-0.03}$	$3.74^{+0.08+0.13}_{-0.08-0.22}$	$2.33^{+0.05+0.08}_{-0.05-0.14}$
	$10^{-11} \times \mathcal{B}r(D^{*+} \rightarrow \eta' \rho^+)$	$10^{-13} \times \mathcal{B}r(D^{*+} \rightarrow \eta' K^{*+})$	$10^{-12} \times \mathcal{B}r(D^{*+} \rightarrow \eta' \pi^+)$	$10^{-14} \times \mathcal{B}r(D^{*+} \rightarrow \eta' K^+)$
This work	$1.41^{+0.03+0.01}_{-0.03-0.03}$	$7.94^{+0.18+0.01}_{-0.17-0.15}$	$1.51^{+0.03+0.03}_{-0.03-0.06}$	$8.01^{+0.18+0.16}_{-0.17-0.35}$
	$10^{-11} \times \mathcal{B}r(D^{*+} \rightarrow \pi^0 \rho^+)$	$10^{-12} \times \mathcal{B}r(D^{*+} \rightarrow \pi^0 K^{*+})$	$10^{-12} \times \mathcal{B}r(D^{*+} \rightarrow \pi^0 \pi^+)$	$10^{-13} \times \mathcal{B}r(D^{*+} \rightarrow \pi^0 K^+)$
This work	$8.27^{+0.18+0.09}_{-0.17-0.08}$	$3.89^{+0.09+0.03}_{-0.08-0.04}$	$7.93^{+0.18+0.14}_{-0.17-0.33}$	$5.19^{+0.11+0.09}_{-0.11-0.22}$
	$10^{-11} \times \mathcal{B}r(D^{*+} \rightarrow \pi^+ \phi)$	$10^{-12} \times \mathcal{B}r(D^{*+} \rightarrow \pi^+ K^0)$		
This work	$1.40^{+0.30+0.11}_{-0.03-0.01}$	$1.06^{+0.02+0.02}_{-0.02-0.04}$		

TABLE VIII: Branching ratios of the non-leptonic decays $D_s^* \rightarrow PM$.

	$10^{-7} \times \mathcal{B}r(D_s^{*+} \rightarrow K^0 \rho^+)$	$10^{-9} \times \mathcal{B}r(D_s^{*+} \rightarrow K^0 K^{*+})$	$10^{-9} \times \mathcal{B}r(D_s^{*+} \rightarrow K^0 \pi^+)$	$10^{-10} \times \mathcal{B}r(D_s^{*+} \rightarrow K^0 K^+)$
This work	$1.17^{+0.13+0.02+0.00}_{-0.10-0.05-0.00}$	$5.33^{+0.58+0.14+0.00}_{-0.47-0.27-0.00}$	$9.38^{+1.02+0.64+0.04}_{-0.78-0.90-0.05}$	$6.07^{+0.66+0.41+0.03}_{-0.50-0.58-0.03}$
	$10^{-6} \times \mathcal{B}r(D_s^{*+} \rightarrow \eta \rho^+)$	$10^{-8} \times \mathcal{B}r(D_s^{*+} \rightarrow \eta K^{*+})$	$10^{-8} \times \mathcal{B}r(D_s^{*+} \rightarrow \eta \pi^+)$	$10^{-9} \times \mathcal{B}r(D_s^{*+} \rightarrow \eta K^+)$
This work	$1.04^{+0.11+0.03+0.00}_{-0.09-0.05-0.00}$	$4.87^{+0.53+0.14+0.00}_{-0.40-0.27-0.00}$	$9.48^{+1.03+0.57+0.03}_{-0.78-0.85-0.02}$	$6.09^{+0.66+0.37+0.02}_{-0.50-0.55-0.01}$
	$10^{-7} \times \mathcal{B}r(D_s^{*+} \rightarrow \eta' \rho^+)$	$10^{-8} \times \mathcal{B}r(D_s^{*+} \rightarrow \eta' K^{*+})$	$10^{-8} \times \mathcal{B}r(D_s^{*+} \rightarrow \eta' \pi^+)$	$10^{-9} \times \mathcal{B}r(D_s^{*+} \rightarrow \eta' K^+)$
This work	$5.90^{+0.64+0.13+0.00}_{-0.49-0.28-0.01}$	$4.65^{+0.51+0.10+0.00}_{-0.38-0.22-0.00}$	$9.05^{+0.99+0.42+0.02}_{-0.75-0.68-0.01}$	$5.14^{+0.56+0.24+0.01}_{-0.42-0.38-0.01}$
	$10^{-8} \times \mathcal{B}r(D_s^{*+} \rightarrow K^+ \phi)$			
This work	$2.41^{+0.26+0.06+0.01}_{-0.21-0.12-0.01}$			

In Tables VII and VIII, we list the branching ratios of the non-leptonic decays $D^* \rightarrow PM$ and $D_s^* \rightarrow PM$, respectively, where the uncertainties arise from the full widths of the charmed mesons $D_{(s)}^*$ and the shape parameters of the initial and final state mesons. Numerically, we adopt the Wilson coefficients $a_1=1.2$ and $a_2=-0.5$ [38]. The following are some comments:

1. The branching ratio of the decay $D_s^{*+} \rightarrow \eta\rho^+$ is four orders of magnitude larger than that of the decay $D^{*+} \rightarrow \eta\rho^+$. It is mainly because that the decay width of the D^{*+} meson $\Gamma_{D^{*+}}$ is about 6.8×10^2 times larger than $\Gamma_{D_s^{*+}}$. Furthermore, the former channel has an enhancement factor $|V_{cs}/V_{cd}|^2 \approx 20$ compared to the latter decay. Although CKM matrix elements of the decay $D^{*0} \rightarrow K^-\rho^+$ are much larger compared with those of the decay $D_s^{*+} \rightarrow K^0 K^{*+}$, the promotion to the branching ratio from the CKM factors is almost canceled out by the large decay width $\Gamma_{D^{*0}}$. So the branching ratios of these two decays are close to each other.
2. The branching ratios of the D^{*0} and D^{*+} decays to the same isospin final states should be almost equal. While the D^{*+} meson decays are dynamically induced by both external and internal W emission interactions, which are destructive each other. This reason induces the hierarchical relationship, $\mathcal{B}r(D^{*+} \rightarrow \bar{K}^0 M) < \mathcal{B}r(D^{*0} \rightarrow K^- M)$ with M referring to π^+, K^+, ρ^+ and K^{*+} . The branching ratios of the decays $D_{(s)}^* \rightarrow PK^*(\rho)$ are always larger than those of the corresponding decays $D_{(s)}^* \rightarrow PK(\pi)$. It is because that there are three partial amplitudes for the former, while only the p-wave amplitude contributes to the latter. It is worth mentioning that our predictions for the branching ratios of the decays $D^{*0} \rightarrow K^-\rho^+$, $D^{*0} \rightarrow K^-\pi^+$, $D^{*+} \rightarrow \bar{K}^0\rho^+$ and $D^{*+} \rightarrow \bar{K}^0\pi^+$ are comparable with the results obtained in the NF approach [38], which are listed in Table VII.
3. It is noticed that some of the non-leptonic D_s^{*+} decay channels are most likely to be observed in the future collider experiments. Especially, the decay $D_s^{*+} \rightarrow \eta\rho^+$ has the largest branching ratio with 10^{-6} order, which will be within the measurement precision and capability of BESIII experiments in the near future.
4. In order to cancel out a large part of the theoretical and experimental uncertainties and SU (3) symmetry breaking effect, it is helpful to consider the ratios of the branching ratios, such as

$$\begin{aligned}
R_{D_s^{*+}}^\eta &\equiv \frac{\mathcal{B}r(D_s^{*+} \rightarrow \eta K^+)}{\mathcal{B}r(D_s^{*+} \rightarrow \eta \pi^+)} = 0.064 \pm 0.011, & R_{D_s^{*+}}^{K^0} &\equiv \frac{\mathcal{B}r(D_s^{*+} \rightarrow K^0 K^+)}{\mathcal{B}r(D_s^{*+} \rightarrow K^0 \pi^+)} = 0.065 \pm 0.012, \\
R_{D^{*+}}^\eta &\equiv \frac{\mathcal{B}r(D^{*+} \rightarrow \eta K^+)}{\mathcal{B}r(D^{*+} \rightarrow \eta \pi^+)} = 0.062_{-0.006}^{+0.004}, & R_{D^{*0}}^{K^-} &\equiv \frac{\mathcal{B}r(D^{*0} \rightarrow K^- K^+)}{\mathcal{B}r(D^{*0} \rightarrow K^- \pi^+)} = 0.063 \pm 0.010,
\end{aligned}$$

where the uncertainties from the transition form factors are cancelled.

The number of potential events associated with the decays $D^{*0} \rightarrow K^-\rho^+, K^-e^+\nu_e$ and $D_s^{*+} \rightarrow \eta\rho^+, \eta e^+\nu_e$, which possess the largest branching ratios in our considered different types of decays, are listed in Table IX. These results indicate that the study of $D_{(s)}^*$ meson weak decays in experiments is feasible.

TABLE IX: The potential event numbers of the decays $D^{*0} \rightarrow K^-\rho^+, K^-e^+\nu_e$ and $D_s^{*+} \rightarrow \eta\rho^+, \eta e^+\nu_e$ in the future experiments, where the available event numbers of the $D_{(s)}^*$ have been estimated in Sec. I.

experiments	SuperKEKB	STCF	CEPC[18]	FCC-ee[19]	HL-LHC
N_{D^*}	2×10^{10}	8×10^{10}	10^{11}	10^{12}	2×10^{14}
$N_{D^{*+} \rightarrow K^-\rho^+}$	102	410	513	5.13×10^3	1.03×10^6
$N_{D^{*+} \rightarrow K^-e^+\nu_e}$	158	634	793	7.93×10^3	1.59×10^6
$N_{D_s^{*+}}$	5.5×10^9	10^{10}	1.3×10^{10}	6.6×10^{10}	4×10^{13}
$N_{D_s^{*+} \rightarrow \eta\rho^+}$	5.72×10^3	1.04×10^4	1.35×10^4	6.86×10^4	3.94×10^7
$N_{D_s^{*+} \rightarrow \eta e^+\nu_e}$	8.03×10^3	1.46×10^4	1.89×10^4	9.63×10^4	5.84×10^7

IV. SUMMARY

Although the D^* and D_s^* mesons were discovered more than 45 years ago, the information about their properties is still relatively limited, especially, the measurements of the $D_{(s)}^*$ weak decays are still unavailable from experiments. Inspired by the recent advances and future prospects for the study of $D_{(s)}^*$ mesons in the collider experiments, we explore both the semi-leptonic and the non-leptonic $D_{(s)}^*$ weak decays. Combining the helicity amplitudes with the form factors of the transitions $D_{(s)}^* \rightarrow \pi, K, \eta_{q,s}$ obtained from the CLFQM, the branching ratios of the corresponding $D_{(s)}^*$ weak decays are calculated. The D^* weak decays can be measured by some of the future collider experiments with the ability to observe the branching ratio with 10^{-9} order, such as the FCC-ee and the HL-LHC. Compared to D^* meson, the D_s^* meson weak decays are relatively easier to be observed by the future experiments. For example, the branching ratios of the decays $D_s^{*+} \rightarrow \eta\ell^+\nu_\ell$ and $D_s^{*+} \rightarrow \eta\rho^+$ can reach up to 10^{-6} order, which correspond to tens of thousands of events in the e^+e^- collider experiments and tens of millions of events at the HL-LHC. Furthermore, in order to provide more detailed physical picture for our considered decays, the longitudinal polarization fraction f_L and the forward-backward asymmetry A_{FB} are also calculated.

Acknowledgment

This work is partly supported by the National Natural Science Foundation of China under Grant No. 11347030, by the Program of Science and Technology Innovation Talents in Universities of Henan Province 14HASTIT037, and the Natural Science Foundation of

Henan Province under grant no. 232300420116. We would like to thank Prof. Junfeng Sun for helpful discussions.

Appendix A: Some specific rules under the p^- integration

When integrating, it is important to include the zero-mode contribution for proper integration in the CLFQM. Specifically, we follow the rules outlined in Refs.[11]

$$\hat{p}'_{1\mu} \doteq P_\mu A_1^{(1)} + q_\mu A_2^{(1)}, \quad (\text{A1})$$

$$\hat{p}'_{1\mu}\hat{p}'_{1\nu} \doteq g_{\mu\nu}A_1^{(2)} + P_\mu P_\nu A_2^{(2)} + (P_\mu q_\nu + q_\mu P_\nu) A_3^{(2)} + q_\mu q_\nu A_4^{(2)}, \quad (\text{A2})$$

$$Z_2 = \hat{N}'_1 + m_1'^2 - m_2^2 + (1 - 2x_1) M'^2 + (q^2 + q \cdot P) \frac{p'_\perp \cdot q_\perp}{q^2}, \quad (\text{A3})$$

$$\hat{p}'_{1\mu}\hat{N}_2 \rightarrow q_\mu \left[A_2^{(1)} Z_2 + \frac{q \cdot P}{q^2} A_1^{(2)} \right], \quad (\text{A4})$$

$$\hat{p}'_{1\mu}\hat{p}'_{1\nu}\hat{N}_2 \rightarrow g_{\mu\nu}A_1^{(2)} Z_2 + q_\mu q_\nu \left[A_4^{(2)} Z_2 + 2 \frac{q \cdot P}{q^2} A_2^{(1)} A_1^{(2)} \right], \quad (\text{A5})$$

$$A_1^{(1)} = \frac{x_1}{2}, \quad A_2^{(1)} = A_1^{(1)} - \frac{p'_\perp \cdot q_\perp}{q^2}, \quad A_3^{(2)} = A_1^{(1)} A_2^{(1)}, \quad (\text{A6})$$

$$A_4^{(2)} = \left(A_2^{(1)} \right)^2 - \frac{1}{q^2} A_1^{(2)}, \quad A_1^{(2)} = -p_\perp'^2 - \frac{(p'_\perp \cdot q_\perp)^2}{q^2}, \quad A_2^{(2)} = \left(A_1^{(1)} \right)^2. \quad (\text{A7})$$

Appendix B: The amplitudes for $D_{(s)}^* \rightarrow PM$ decays

$$\begin{aligned}
S_{\mu\nu}^{D_{(s)}^*P} &= \left(S_V^{D_{(s)}^*P} - S_A^{D_{(s)}^*P} \right)_{\mu\nu} \\
&= \text{Tr} \left[\left(\gamma_\nu - \frac{1}{W_V''} (p_1'' - p_2)_\nu \right) (p_1'' + m_1'') (\gamma_\mu - \gamma_\mu \gamma_5) (\not{p}_1' + m_1') \gamma_5 (-\not{p}_2 + m_2) \right] \\
&= -2i\epsilon_{\mu\nu\alpha\beta} \{ p_1'^\alpha P^\beta (m_1'' - m_1') + p_1'^\alpha q^\beta (m_1'' + m_1' - 2m_2) + q^\alpha P^\beta m_1' \} \\
&\quad + \frac{1}{W_V''} (4p_{1\nu}' - 3q_\nu - P_\nu) i\epsilon_{\mu\alpha\beta\rho} p_1'^\alpha q^\beta P^\rho \\
&\quad + 2g_{\mu\nu} \{ m_2 (q^2 - N_1' - N_1'' - m_1'^2 - m_1''^2) - m_1' (M''^2 - N_1'' - N_2 - m_1''^2 - m_2^2) \\
&\quad - m_1'' (M'^2 - N_1' - N_2 - m_1'^2 - m_2^2) - 2m_1' m_1'' m_2 \} \\
&\quad + 8p_{1\mu}' p_{1\nu}' (m_2 - m_1') - 2(P_\mu q_\nu + q_\mu P_\nu + 2q_\mu q_\nu) m_1' + 2p_{1\mu}' P_\nu (m_1' - m_1'') \\
&\quad + 2p_{1\mu}' q_\nu (3m_1' - m_1'' - 2m_2) + 2P_\mu p_{1\nu}' (m_1' + m_1'') + 2q_\mu p_{1\nu}' (3m_1' + m_1'' - 2m_2) \\
&\quad + \frac{1}{2W_V''} (4p_{1\nu}' - 3q_\nu - P_\nu) \{ 2p_{1\mu}' [M'^2 + M''^2 - q^2 - 2N_2 + 2(m_1' - m_2)(m_1'' + m_2)] \\
&\quad + q_\mu [q^2 - 2M'^2 + N_1' - N_1'' + 2N_2 - (m_1 + m_1'')^2 + 2(m_1' - m_2)^2] \\
&\quad + P_\mu [q^2 - N_1' - N_1'' - (m_1' + m_1'')^2] \}. \tag{B1}
\end{aligned}$$

The following formulas are the analytical expressions of the form factors of transitions $D_{(s)}^* \rightarrow P$ in the covariant light-front quark model

$$\begin{aligned}
V^{D_{(s)}^*P}(q^2) &= \frac{N_c(M' + M'')}{16\pi^3} \int dx_2 d^2 p_\perp \frac{2h_{D_{(s)}^*}' h_P''}{x_2 \hat{N}_1' \hat{N}_1''} \left\{ x_2 m_1' + x_1 m_2 + (m_1' - m_1'') \frac{p_\perp' \cdot q_\perp}{q^2} \right. \\
&\quad \left. + \frac{2}{w_{D_{(s)}^*}''} \left[p_\perp'^2 + \frac{(p_\perp' \cdot q_\perp)^2}{q^2} \right] \right\}, \tag{B2}
\end{aligned}$$

$$\begin{aligned}
A_0^{D_{(s)}^*P}(q^2) &= \frac{M' + M''}{2M''} A_1^{D_{(s)}^*P}(q^2) - \frac{M' - M''}{2M''} A_2^{D_{(s)}^*P}(q^2) - \frac{q^2}{2M''} \frac{N_c}{16\pi^3} \int dx_2 d^2 p_\perp \frac{h_{D_{(s)}^*}' h_P''}{x_2 \hat{N}_1' \hat{N}_1''} \{ 2(2x_1 - 3) \\
&\quad (x_2 m_1' + x_1 m_2) - 8(m_1' - m_2) \times \left[\frac{p_\perp'^2}{q^2} + 2 \frac{(p_\perp' \cdot q_\perp)^2}{q^4} \right] - [(14 - 12x_1) m_1' \\
&\quad - 2m_1'' - (8 - 12x_1) m_2] \frac{p_\perp' \cdot q_\perp}{q^2} + \frac{4}{w_{D_{(s)}^*}''} ([M'^2 + M''^2 - q^2 + 2(m_1' - m_2)(m_1'' + m_2)] \\
&\quad \times (A_3^{(2)} + A_4^{(2)} - A_2^{(1)}) + Z_2 (3A_2^{(1)} - 2A_4^{(2)} - 1) + \frac{1}{2} [x_1 (q^2 + q \cdot P) - 2M'^2 - 2p_\perp' \cdot q_\perp \\
&\quad - 2m_1' (m_1'' + m_2) - 2m_2 (m_1' - m_2)] (A_1^{(1)} + A_2^{(1)} - 1) q \cdot P \left[\frac{p_\perp'^2}{q^2} + \frac{(p_\perp' \cdot q_\perp)^2}{q^4} \right] \\
&\quad \times (4A_2^{(1)} - 3) \} \}, \tag{B3}
\end{aligned}$$

$$\begin{aligned}
A_1^{D(s)P}(q^2) = & -\frac{1}{M' + M''} \frac{N_c}{16\pi^3} \int dx_2 d^2 p'_\perp \frac{h'_{D(s)} h''_P}{x_2 \hat{N}'_1 \hat{N}''_1} \left\{ 2x_1 (m_2 - m'_1) (M_0'^2 + M_0''^2) - 4x_1 m''_1 M_0'^2 \right. \\
& + 2x_2 m'_1 q \cdot P + 2m_2 q^2 - 2x_1 m_2 (M'^2 + M''^2) + 2(m'_1 - m_2) (m'_1 + m''_1)^2 + 8(m'_1 - m_2) \\
& \times \left[p'^2_\perp + \frac{(p'_\perp \cdot q_\perp)^2}{q^2} \right] + 2(m'_1 + m''_1) (q^2 + q \cdot P) \frac{p'_\perp \cdot q_\perp}{q^2} - 4 \frac{q^2 p'^2_\perp + (p'_\perp \cdot q_\perp)^2}{q^2 w''_{D(s)}} \\
& \times \left[2x_1 (M'^2 + M_0'^2) - q^2 - q \cdot P - 2(q^2 + q \cdot P) \frac{p'_\perp \cdot q_\perp}{q^2} - 2(m'_1 - m''_1) (m'_1 - m_2) \right] \Big\}, \quad (B4)
\end{aligned}$$

$$\begin{aligned}
A_2^{D(s)P}(q^2) = & \frac{N_c(M' + M'')}{16\pi^3} \int dx_2 d^2 p'_\perp \frac{2h'_{D(s)} h''_P}{x_2 \hat{N}'_1 \hat{N}''_1} \left\{ (x_1 - x_2) (x_2 m'_1 + x_1 m_2) - \frac{p'_\perp \cdot q_\perp}{q^2} [2x_1 m_2 + m''_1 \right. \\
& + (x_2 - x_1) m'_1] - 2 \frac{x_2 q^2 + p'_\perp \cdot q_\perp}{x_2 q^2 w''_{D(s)}} [p'_\perp \cdot p''_\perp + (x_1 m_2 + x_2 m'_1) (x_1 m_2 - x_2 m''_1)] \Big\}. \quad (B5)
\end{aligned}$$

-
- [1] M. V. Terentev, Sov. J. Nucl. Phys. **24**, 106 (1976).
[2] V. B. Berestetsky and M. V. Terentev, Sov. J. Nucl. Phys. **25**, 347 (1977).
[3] W. Jaus, Phys. Rev. D **41**, 3394 (1990).
[4] W. Jaus, Phys. Rev. D **44**, 2851 (1991).
[5] H. M. Choi and C. R. Ji, Phys. Lett. B **460**, 461 (1999) [arXiv:hep-ph/9903496].
[6] W. Jaus, Phys. Rev. D **60**, 054026 (1999).
[7] Z. Q. Zhang, Z. J. Sun, Y. C. Zhao, Y. Y. Yang and Z. Y. Zhang, Eur. Phys. J. C **83**, 477 (2023) [arXiv:2301.11107 [hep-ph]].
[8] Y. Y. Yang, Z. Q. Zhang, H. Yang, Z. J. Sun and M. X. Xie, Phys. Rev. D **110**, 033006 (2024) [arXiv:2405.00496 [hep-ph]].
[9] W. Wang, Y. L. Shen and C. D. Lu, Phys. Rev. D **79**, 054012 (2009) [arXiv:0811.3748 [hep-ph]].
[10] H. W. Ke, T. Liu and X. Q. Li, Phys. Rev. D **89**, 017501 (2014) [arXiv:1307.5925 [hep-ph]].
[11] H. Y. Cheng, C. K. Chua and C. W. Hwang, Phys. Rev. D **69**, 074025 (2004) [arXiv:hep-ph/0310359].
[12] X. X. Wang, W. Wang and C. D. Lu, Phys. Rev. D **79**, 114018 (2009) [arXiv:0901.1934 [hep-ph]].
[13] M. Ablikim *et al.* (BESIII Collaboration), Phys. Rev. Lett. **131**, 141802 (2023) [arXiv:2304.12159 [hep-ex]].
[14] M. Ablikim *et al.* (BESIII Collaboration), JHEP **05**, 155 (2022) [arXiv:2112.06477 [hep-ex]].
[15] X. R. Lyu (STCF Working group), PoS **BEAUTY2020**, 060 (2021).
[16] M. Lisovyi, A. Verbytskyi, O. Zenaiev, Eur. Phys. J. C **76**, 397 (2016) [arXiv:1509.01061 [hep-ex]].

- [17] E. Kou *et al.* (Belle-II), Prog. Theor. Exp. Phys. **2019**, 123C01 (2019) [erratum:PTEP **2020**, 029201 (2020)] [arXiv:1808.10567 [hep-ex]].
- [18] J. B. Guimarães da Costa *et al.* (CEPC Study Group), IHEP-CEPC-DR-2018-02 [arXiv:1811.10545 [hep-ex]].
- [19] A. Abada *et al.*, Eur. Phys. J. C **79**, 474 (2019).
- [20] P. Zyla *et al.* (Particle Data Group), Prog. Theor. Exp. Phys. **2020**, 083C01 (2020).
- [21] R. Aaij *et al.* (LHCb Collaboration), JHEP **03**, 159 (2016) [erratum: JHEP **09**, 013 (2016); erratum: JHEP **05**, 074 (2017)] [arXiv:1510.01707 [hep-ex]].
- [22] R. Aaij *et al.* (LHCb Collaboration) [arXiv:1808.08865 [hep-ex]].
- [23] X. K. Dong, L. L. Wang, C. Z. Yuan, Chin. Phys. C **42**, 043002 (2018) [arXiv:1808.08865 [hep-ex]].
- [24] G. Pakhlova *et al.* (Belle Collaboration), Phys. Rev. D **83**, 011101 (2011) [arXiv:1711.07311 [hep-ph]].
- [25] P. Sanchez *et al.* (BaBar Collaboration), Phys. Rev. D **82**, 052004 (2010) [arXiv:1008.0338 [hep-ex]].
- [26] A. Abada *et al.*, Eur. Phys. J. Special Topics **228**, 1109 (2019).
- [27] Z. J. Sun, Z. Q. Zhang, Y. Y. Yang and H. Yang, Eur. Phys. J. C **84**, 65 (2024) [arXiv:2311.04431 [hep-ph]].
- [28] H. Y. Cheng and C. K. Chua, Phys. Rev. D **69**, 094007 (2004) [erratum: Phys. Rev. D **81**, 059901 (2010)] [arXiv:hep-ph/0401141].
- [29] C. W. Hwang and Z. T. Wei, J. Phys. G **34**, 687 (2007) [arXiv:hep-ph/0609036].
- [30] C. D. Lu, W. Wang and Z. T. Wei, Phys. Rev. D **76**, 014013 (2007) [arXiv:hep-ph/0701265].
- [31] W. Wang, Y. L. Shen and C. D. Lu, Eur. Phys. J. C **51**, 841 (2007) [arXiv:0704.2493 [hep-ph]].
- [32] Y. M. Wang, H. Zou, Z. T. Wei, X. Q. Li and C. D. Lu, Eur. Phys. J. C **54**, 107 (2008) [arXiv:0707.1138 [hep-ph]].
- [33] Y. M. Wang, H. Zou, Z. T. Wei, X. Q. Li and C. D. Lu, Eur. Phys. J. C **55**, 607 (2008) [arXiv:0802.2762 [hep-ph]].
- [34] R. Dhir, R. Verma and A. Sharma, Adv. High Energy Phys, **2013**, 706543 (2013)[arXiv:0903.1201 [hep-ph]].
- [35] T. Wang, Y. Jiang, H. Yuan, K. Chai and G. L. Wang, J. Phys. G **44**, 045004 (2017)[arXiv:1604.03298 [hep-ph]].
- [36] Y. Sakaki, M. Tanaka, A. Tayduganov and R. Watanabe, Phys. Rev. D **88**, 094012 (2013)[arXiv:1309.0301 [hep-ph]].
- [37] T. Feldmann, P. Kroll and B. Stech, Phys. Rev. D **58**, 114006 (1998) [arXiv:hep-ph/9802409].
- [38] Y. L. Yang, K. Li, Z. L. Li, J. S. Huang, Q. Chang and J. F. Sun, Phys. Rev. D **106**, 036029

- (2022)[arXiv:2207.10277 [hep-ph]].
- [39] G. L. Yu, Z. Y. Li, Z. G. Wang, Eur. Phys. J. C **75**, 243 (2015) [arXiv:1502.01698 [hep-ph]].